

available at [www.sciencedirect.com](http://www.sciencedirect.com)journal homepage: [www.intl.elsevierhealth.com/journals/dema](http://www.intl.elsevierhealth.com/journals/dema)

## Bond strength and interfacial characterization of eight low fusing porcelains to cp Ti

S. Zinelis<sup>a,\*</sup>, X. Barmpagadaki<sup>b,1</sup>, V. Vergos<sup>c</sup>, M. Chakmakchi<sup>a</sup>, G. Eliades<sup>a</sup>

<sup>a</sup> Department of Biomaterials, School of Dentistry, University of Athens, 2 Thivon Str, Goudi 115 27, Athens, Greece

<sup>b</sup> Private practice, Athens, Greece

<sup>c</sup> Department of Dental Technology, School of Health and Care Profession, Technological Educational Institution of Athens, Athens, Greece

### ARTICLE INFO

#### Article history:

Received 5 June 2009

Received in revised form

24 September 2009

Accepted 5 November 2009

#### Keywords:

Metal–ceramic

Ti porcelain

Three point bending

SEM/EDS

Interfacial characterization

### ABSTRACT

**Objectives.** The aim of this study was the interfacial characterization and the determination of bond strength of commercially available low fusing dental porcelain for Ti.

**Methods.** Eight materials were included in this study: Duceratin, Duceratin Plus, Initial Ti, Ti-22, TiKrom, TitanKeramik, Triceram (powder) and Triceram (paste). Eight ISO 9693 bond characterization specimens from each porcelain were prepared according to manufacturers' instructions. One specimen from each group was embedded in acrylic resin and after metallographic preparation was studied under an SEM. Interfacial characterization was carried out with Backscattered Electron Imaging and X-ray EDS analysis operating in line scan mode. Metal–ceramic specimens were tested in three point bending at a crosshead speed of 1.5 mm/min according to ISO 9693 requirements. Additionally the fracture mode (adhesive–cohesive) of all specimens was evaluated employing SEM/EDS analysis. The results of bond strength and adhesive percentage were statistically analysed with one-way ANOVA and SNK multiple comparison test ( $\alpha=0.05$ ). Additionally the possible correlation between the bond strength and fracture mode was also tested using Pearson test.

**Results.** Interfacial characterization showed the mutual diffusion of Ti, Si, O and La along the Ti–ceramic interface. Only in Tricerap (paste) Zr showed an increased concentration at the interface. The results of bond strength classified the materials in the following decreasing order: TiKrom > Duceratin > Initial Ti > Duceratin Plus > Ti-22 > Triceram(paste) > Triceram(powder) > TitanKeramik. No correlation ( $r=0.132$ ) between the fracture mode and bond strength of the selected material denoting that the fracture mode is irrelevant with the bond strength of Ti–ceramic joint and thus the former should not be applied for comparison among different materials.

**Significance.** According to the results of this study the materials tested provided great difference in interfacial analysis and bond strength with metallic Ti.

© 2009 Academy of Dental Materials. Published by Elsevier Ltd. All rights reserved.

## 1. Introduction

During recent decades, commercially pure titanium (cp Ti) has been used in dentistry [1–6] for metal–ceramic restorations because of its excellent biocompatibility, good corrosion resistance, and adequate mechanical properties [7–9].

\* Corresponding author. Tel.: +30 2107461102; fax: +30 2107461306.

E-mail address: [szinelis@dent.uoa.gr](mailto:szinelis@dent.uoa.gr) (S. Zinelis).

<sup>1</sup> Commercial Dental Technician.

**Table 1 – The commercial names, the firing temperature and the coefficient of thermal expansion (CTE) of the porcelains tested as provided by the manufacturers.**

Brand names	Material type	Manufacturers	Firing temp. (°C)	CTE ( $\times 10^{-6} \text{ K}^{-1}$ )
Duceratin	Powder	Degussa Dental, Hanau, Germany	830	N/A <sup>a</sup>
Duceratin plus	Powder	Degussa Dental, Hanau, Germany	780	12.5 (25–500 °C)
Initial Ti	Powder	GC Corporation, Tokyo, Japan.	810	N/A <sup>b</sup>
Ti-22	Powder	Noritake, Nagoya, Japan	800	9.7~10.7 (25–500 °C)
TiKrom	Powder	Orotig, Verona, Italy	810	N/A <sup>a</sup>
Titankeramik	Paste	Vita, Bad Sackingen, Germany	800	N/A <sup>a</sup>
Triceram	Powder	Esprident-Dentaurum, Ispringen, Germany	795	9.4~9.5 <sup>b</sup>
Triceram	Paste	Esprident-Dentaurum, Ispringen, Germany	795	9.2 (25–400 °C)

<sup>a</sup> Not available

<sup>b</sup> Temperature range is not provided

Strong bonding of porcelain to cp Ti is critical for the longevity of metal–ceramic restorations [10]. Contrary to conventional alloys, Ti is rapidly oxidized during porcelain firing at temperatures above 800 °C providing a thick and non-adherent layer of Ti oxide [11–13], that compromises the metal–ceramic bond strength compared to conventional dental alloys [14–16] increasing the risk of failure [1,2,4–6,17]. Various surface treatments have been introduced to overcome this limitation such as surface roughening [18,19], preoxidation [20], etching [21,22], and the application of bonding coatings [23–25]. However, only the roughening of metallic surface prior to porcelain application has been adopted as a standard operating procedure [26].

Although extensive research has been done for the evaluation of metal–ceramic bond strength of low fusing porcelains to cp Ti in most cases the results are not directly comparable due to the great differences in the research protocols employed. In the relevant literature more than fifteen different metal–ceramic bond strength tests [27] have been used and the results have been reported in three different ways including debonding load (Nt) [15], bond strength in MPa [14,16,28] and fracture mode [21,23,29] as percentage of cohesive and adhesive failures. The most recent specification on assessment of metal–ceramic bonding of the International Standardization Organization ISO 9693 [30] provides a sound method for the standardized evaluation of bond strength of metal–ceramic systems and meets the criteria for a comparative evaluation of metal–ceramic bond strength, independently from the mechanical properties of alloys tested.

The aim of the present study was to evaluate the compliance of eight commercially available dental porcelains for veneering cp Ti with ISO 9693:1999 specification and to characterize the morphology and elemental composition of the metal–ceramic interfaces.

## 2. Materials and methods

### 2.1. Specimens preparation

Seventy rectangular wax (Anutex; Kemdent Dental Products Ltd, Wiltshire, United Kingdom) pattern (30 mm  $\times$  3.5 mm  $\times$  1 mm) were invested with magnesia based investment material (Titavest CB, Morita, Kyoto, Japan) and casting were performed with grade II cp Ti (J. Morita Co., Kyoto, Japan) in a two chamber inert-gas vacuum pressure

casting machine (Cyclarc II, Morita, Kyoto Japan). Castings were sandblasted with 110  $\mu\text{m}$  alumina oxide particles ( $\text{Al}_2\text{O}_3$ ) for the removal of the investment material. The porosity of all specimens was examined radiographically. A dental radiographic unit (Gendex 756 DC; Dentsply, Milano, Italy) was used under the following conditions: 65 kV accelerating voltage 7 mA beam current, 13 cm distance from the source to charged couple device sensor and 0.8 s exposure time. The specimens with internal pores were excluded from the study. The selected specimens were ground on all sides with 600 grit SiC paper under continuous water cooling in a grinding/polishing machine (Ecomt III, Buehler Bluff Lake, Ill). All specimens were ground up to final dimensions of 25 mm  $\times$  3 mm  $\times$  0.45–0.55 mm. Then one side of each specimen was ground up to 2000 grit and polished with 6  $\mu\text{m}$ , diamond paste (DP Paste, Struers, Copenhagen, Denmark). Before the porcelain application final cleaning was performed with hot distilled water in ultrasonic cleaner for 10 min. Fifty six specimens were randomly divided in eight groups and the specimens of each group were covered with the porcelains shown in Table 1 according to their manufacturers' instructions. Metallic surface preparation (sandblasting with  $\text{Al}_2\text{O}_3$  particles) and successive porcelain layers (bonding agent, opaque, dentin and glaze) were applied at the center of each specimen over an 8 mm length and 1 mm thickness. One specimen from each group to be used for interfacial analysis was covered with porcelain without prior sandblasting contrary to manufacturers' instructions. To minimize the effect of handling variations, all the metal–ceramic specimens were prepared by one dental technician (the second author).

### 2.2. Interfacial characterization

One specimen from each group was embedded in an acrylic resin (Durofix-2, Struers). After 24 h storage in room temperature the specimens were ground with silicon carbide papers (220–2000 grit size) under continuous water cooling. Final polishing was performed with 0.25  $\mu\text{m}$  diamond paste (DP Paste, Struers) in the grinding/polishing machine (Ecomet III, Buehler, Lake Bluff, IL, USA). The specimens were ultrasonically cleaned for 10 min in a water bath and sputter-coated with carbon in a sputter-coating unit (SCD 004 Sputter-Coater with OCD 30 attachment, Bal-Tec, Vaduz, Liechtenstein). The metal–ceramic interface was examined in

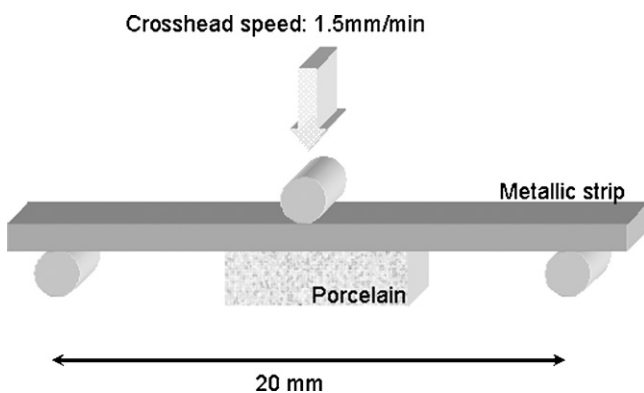


**Fig. 1 – Three point bending of a metal–ceramic specimen according to ISO 9693:1999. The loading was applied on the metallic strip with a crosshead speed of 1.5 mm/min while the distance between the supporting points is 20 mm.**

a scanning electron microscope (Quanta 200, FEI, Hillsboro, Or, USA) equipped with a super ultra-thin Be window X-ray EDS detector (Sapphire CDU, Edax Int, Mahwah, NJ, USA). Interfaces were imaged with Backscattered Electron Imaging (BEI) employing a solid state backscattered detector under 30 kV acceleration voltage, 110  $\mu$ A beam current and 1500 $\times$  nominal magnification. Additionally, the elemental distribution across the metal–ceramic interface was determined by using line scan EDS analysis. The interface was imaged in 30,000 $\times$  magnification and the data were collected across a 8.36  $\mu$ m line each side the metal–ceramic interface employing 14 point of analysis per micron. The results were smoothed employing the Genesis 5.1 software (Edax Int, Mahwah, NJ, USA).

### 2.3. Evaluation of bond strength

Three cast specimens without porcelain were subjected to a three point bending test to determine the modulus of elasticity of cp Ti castings, using a universal testing machine (Tensometer10, Monsanto, Swindon, UK). The specimens were loaded at the center with a crosshead speed of 1.5 mm/min, and the deflection and load were continuously recorded. The elastic modulus of Ti in bending was determined according to the following formula:

$$E = \frac{L^3 \Delta P}{4bh^3 \Delta d}$$

where  $E$  is the elastic modulus in bending,  $L$  is the span between supporting rods (20 mm),  $b$  is the specimen width (3 mm),  $h$  is the specimen thickness (0.5 mm), and  $\Delta P$  and  $\Delta d$  are the load and deflection increment, respectively, between two specific points in the elastic portion of the curve. The remaining six metal–ceramic specimens of each group were loaded in the three point bending device at the same crosshead speed of 1.5 mm/min (Fig. 1). Porcelain debonding was determined by a sudden decrease in the load–deflection graphs. The debonding load was recorded, and the metal–ceramic bond strength in units of MPa was calculated according to the following formula provided by ISO 9693

[30]:

$$\text{Bond strength} = F \times k$$

where  $F$  is the debonding load (Nt), and  $k$  is a coefficient calculated from the ISO specification that is dependent on the modulus of elasticity of the alloy and height of each specimen.

### 2.4. Fracture mode analysis

The metallic fractured surfaces of all specimens were sputter-coated with carbon in a sputter-coating unit (SCD 004 Sputter-Coater with OCD 30 attachment, Bal-Tec, Vaduz, Liechtenstein). The fractured surfaces were examined in SEM employing secondary electron images (SEI) under 25 kV accelerating voltage 110  $\mu$ A beam current and 100 $\times$  nominal magnification. One EDS spectrum was obtained from the central region of each specimen under 30 kV accelerating voltage 100  $\mu$ A beam current and 1.28 mm  $\times$  1.28 mm sampling window. Quantitative analysis was performed in standardless mode using the Genesis (5.1 version) software. (Edax Int). The area fraction of the adherent bonding agent residues (AFBA) on each specimen after porcelain debonding was calculated by the following equation [21]:

$$\% \text{ porcelain adherence} = 100 \times \left[ \frac{Si_f - Si_t}{Si_p - Si_t} \right]$$

where  $Si_f$  is the weight percent of silicon on the specimen surface after porcelain fracture,  $Si_p$  is the weight percent of silicon on the specimen surface covered with opaque porcelain, and  $Si_t$  is the weight percent silicon on the Ti surface before the porcelain firing. In the case of TiKrom and Initial Ti the concentration of La was used instead of Si.

### 2.5. Statistical analysis

The results of bond strength and fracture mode were statistically analysed one-way ANOVA and SNK multiple comparison test ( $\alpha=0.05$ ). To reveal the strength of association between bond strength and fracture mode Pearson correlation procedure was applied.

## 3. Results

### 3.1. Interfacial characterization

Backscattered Electron Images (BEI) from the interface of all materials tested with Ti are presented in Fig. 2. These greyscale images provide information of mean atomic number contrast. In four cases (2c, 2e, 2f and 2h) the zone of bonding agent is clearly distinguished between the Ti and opaque layer. Based on imaged contrast all bonding agents seem to be multiphase materials expect from the bonding agent of TitanKeramik (Fig. 2f), that demonstrated excessive porosity. Additionally in Fig. 2a, b, d and g distinct zones of lower mean atomic number compared to Ti (pointed by the arrows) were observed along the Ti–ceramic interface. Fig. 3 shows the results from the line scan EDS analysis of the materials tested. Ti depicted a progressively reduction from metal to bonding agent, while Si and O showed the inverse behaviour. In Initial Ti (Fig. 3c) O demon-

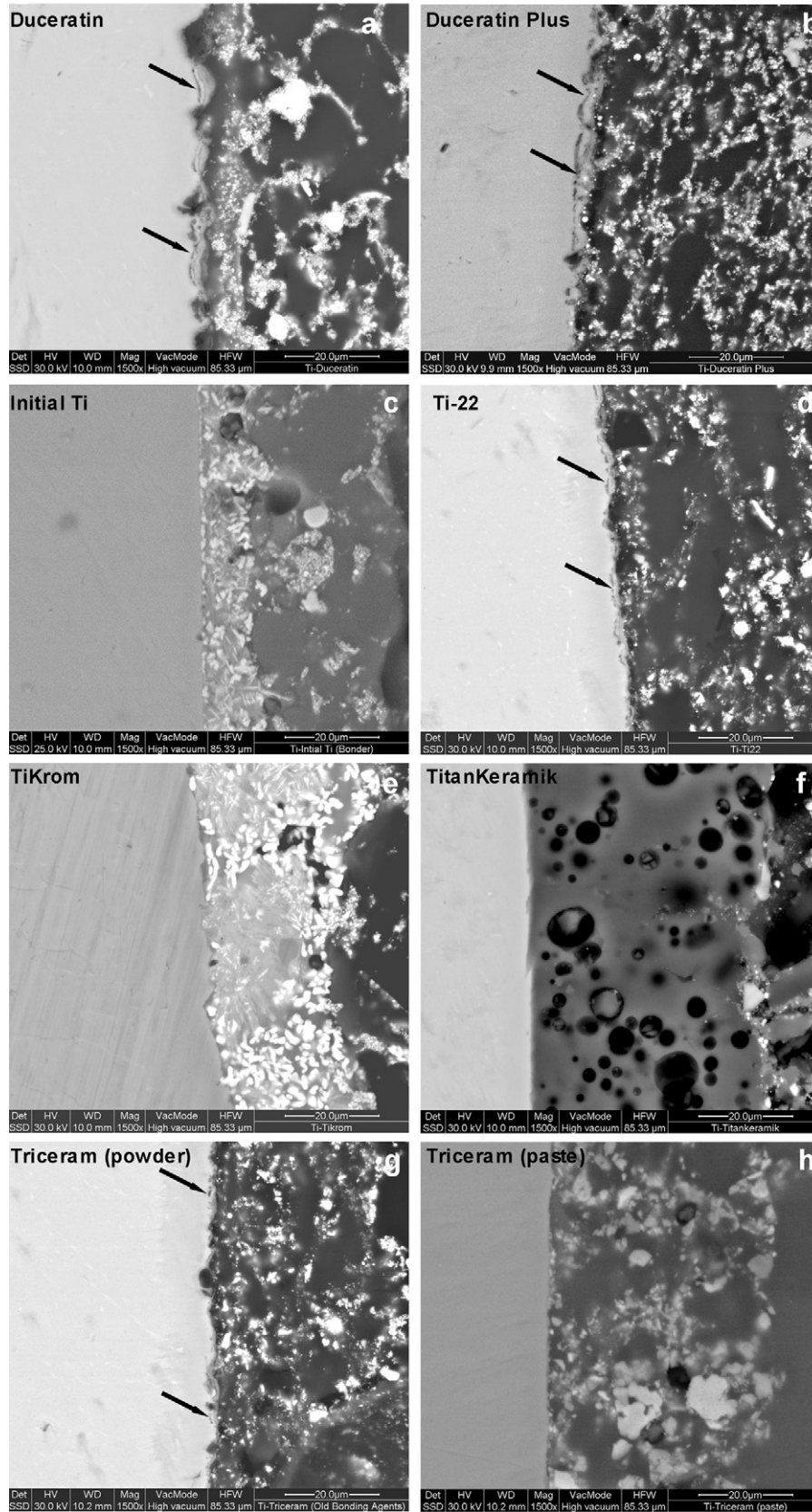


**Fig. 2 – Backscattered Electron Images of the Ti–porcelain interfaces for the materials tested. (a) Duceratin, (b) Duceratin Plus, (c) Initial Ti, (d) Ti-22, (e) TiKrom, (f) TitanKeramik, (g) Triceram (powder) and (h) Triceram (paste). In four cases (c, e, f and h) the zone of bonding agent is clearly distinguished between the Ti (left white region) and the opaque layer. The width of bonding agent zone is estimated approximately 10  $\mu\text{m}$  for Initial Ti (c), 20  $\mu\text{m}$  for Tikrom (e), 40  $\mu\text{m}$  for TitanKeramik (f) and Triceram paste (h). A distinct zone with lower mean atomic number are pointed by the arrows in (a), (b), (d) and (g).**

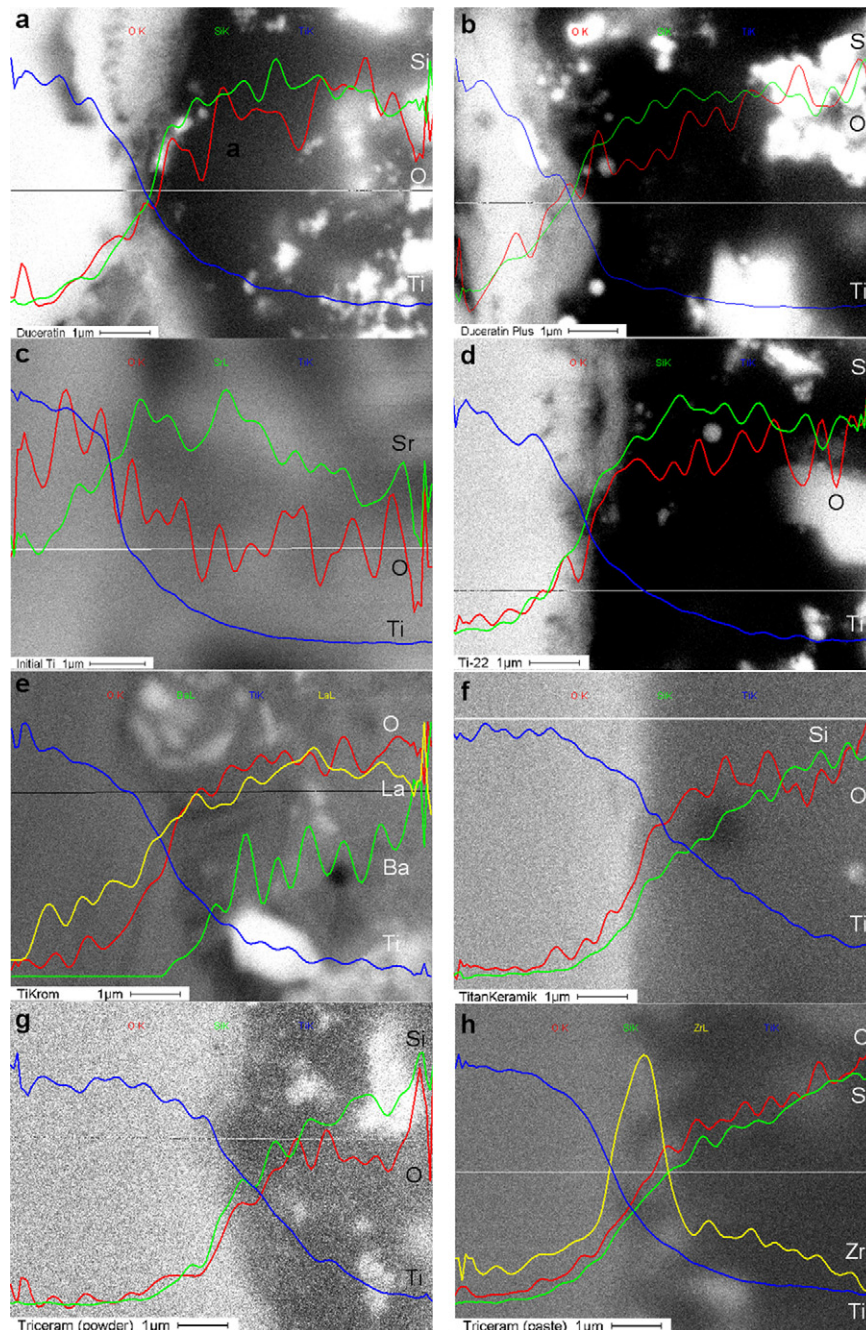


**Fig. 3 – Line scan EDS analysis demonstrating the variation of each element from Ti toward the bonding agent (30,000 $\times$ ). The horizontal line denotes the directions of analysis. (a) Duceratin, (b) Duceratin Plus, (c) Initial Ti, (d) Ti-22, (e) TiKrom, (f) TitanKeramik, (g) Triceram (powder) and (h) Triceram (paste). Line scans have been expanded in y-axis for the sake of clarity and thus should not be used for quantitative comparisons among elements.**

stated an almost steady concentration while Zr showed high concentration at the interface of Ti–Triceram (paste) (Fig. 3h).

### 3.2. Bond strength

A typical load–deflection curve under three point bending is illustrated in Fig. 4. The sudden decrease in loading denotes porcelain debonding. The bond strength results are presented in Table 2 in decreasing order.

### 3.3. Fracture mode

Representative secondary electron images (SEI) from fractured surfaces of Ti–ceramic specimens are presented in Fig. 5. Duceratin, Duceratin Plus, Triceram (powder) Triceram (paste) and Ti-22 demonstrated mainly adhesive fracture at Ti–ceramic interface (Fig. 5a). Initial Ti exhibited predominantly cohesive fracture within bonding agent (Fig. 5b) while TiKrom showed cohesive fracture within bonding agent and

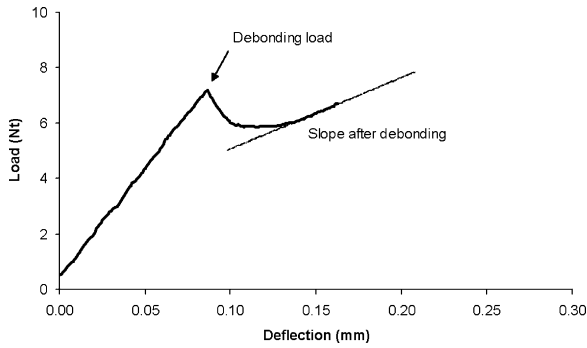


**Fig. 4 – Representative load–deflection curve from three point bending of metal–ceramic specimens. The abrupt decrease in load denotes debonding of ceramic layer. Note the difference in slope after debonding where only the metallic is loaded.**

opaque layers (Fig. 5c). TitanKeramik depicted cohesive fracture within bonding agent with extensive presence of open pores (Fig. 5d). The quantitative results of the failure mode analysis of cohesive–adhesive are shown in Table 3. Fig. 6 presents a plot of the bond strength versus the percentage of cohesive fracture data for each material along with the correlation coefficient ( $r = 0.132$ ). There was no correlation between

**Table 2 – Results of bond strength measurements. The same letters in SNK grouping denotes the mean values without statistical significant differences ( $p > 0.05$ ).**

Material	Bond strength (MPa)	SNK grouping
TiKrom	45 ± 5	A
Duceratin	42 ± 8	A
Initial Ti	31 ± 5	B
Duceratin plus	31 ± 3	B
Ti-22	29 ± 5	BC
Triceram (paste)	28 ± 3	C
Triceram (powder)	21 ± 4	C
Titankeramik	21 ± 3	C

**Table 3 – Results of percentage of cohesive fracture (AFBP) within porcelain layer. The same letters in SNK grouping denotes the mean values without statistical significant differences ( $p > 0.05$ ).**

Material	AFBP (%)	SNK grouping
Tikrom	88.0 ± 5.2	A
Titankeramik	83.3 ± 2.1	A
Initial Ti	67.1 ± 2.8	B
Duceratin	4.6 ± 2.5	C
Triceram (paste)	4.5 ± 1.1	C
Triceram (powder)	3.8 ± 1.4	D
Ti-22	1.2 ± 0.9	E
Duceratin Plus	0.7 ± 0.2	F

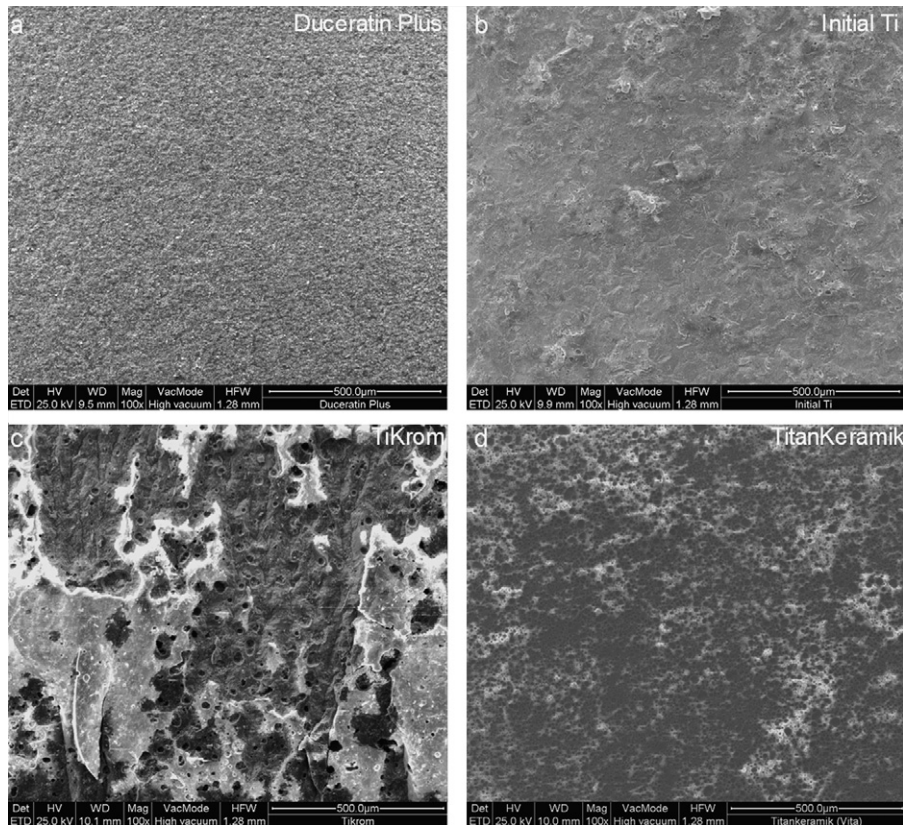


**Fig. 5 – Secondary electron images (SEI) from the metallic fractured surfaces of Ti–ceramic specimens (100×). (a) A representative image of adhesive fracture at Ti–ceramic interface Duceratin, Duceratin Plus, Triceram (powder), Triceram (paste) and Ti-22. (b) Cohesive fracture within ceramic layer of Ti–Initial Ti specimens. (c) Cohesive fracture of Ti–TiKrom specimens. Darker regions are appended to cohesive fracture within bonding agent and lighter to opaque layer. (d) Cohesive fracture within the bonding agent of TitanKeramik with excessive porosity.**

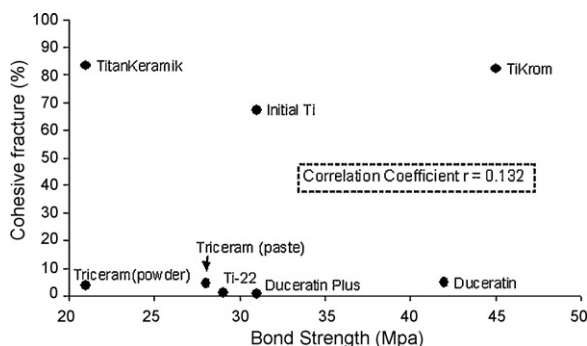


**Fig. 6 – There are no significant relationships between any pair of variables in the correlation table between cohesive fracture and bond strength ( $p > 0.050$ ).**

the bond strength and the fracture mode of materials included in this study.

### 3.4. Discussion

Contrary to manufacturers' instructions (sandblasting with  $Al_2O_3$  particles) for Ti surface preparation before the application of bonding agent the surface of specimens used in this study for interfacial analysis was only metallographically ground and polished. This was done deliberately in order to facilitate the location of interface especially in high magnifications and to avoid the surface contamination of  $Al_2O_3$  particles retained on the surface after sandblasting. These particles masking the real surface distribution of Al and O content at the Ti–porcelain interface.

In four cases (Duceratin, Duceratin Plus, Ti-22, and Triceram powder) a zone with lower atomic number compared to Ti, along the Ti–porcelain interface was found (Fig. 2). These findings are in accordance with previous studies [14,31,32] where this zone has been associated with subsurface oxidation during firing. Although this is a logical assumption it requires further analysis. These four bonding agents have two common characteristics. They are all  $SiO_2$ -based [33] and they are delivered in powder form. These materials are mixed with an aqueous solution producing a slurry that is applied and fired on Ti surface. Therefore, a possible mechanism for Ti subsurface oxidation could be that Ti has enough time to be oxidized before the particles sintered providing a protective layer. This mechanism is also supported by the fact that subsurface oxidation did not occur in paste type  $SiO_2$ -based [33] bonding agents TitanKeramik (Fig. 2f) and Triceram (paste) (Fig. 2h) where probably an organic substance is used as binder. It also profound from the cross section images that the width of bonding agent region varies significantly among materials possibly due to differences in viscosity and contraction during firing. Although all bonding agents presented a few pores, TitanKeramik demonstrated excessive porosity with a random distribution that is in agreement with previous studies [32,34] and might be attributed to the burn out of the organic phase of the bonding agent during firing.

Line scan analysis provided interesting information on the mutual elemental diffusion at the Ti–ceramic interface. In all cases the decreasing in Ti composition starting 1–2  $\mu m$  below

the interface as it appeared in BEI while the porcelain elements (Si, O and La) exhibited inverse distribution, a finding that is in full accordance with the results of previous research [32]. This finding denotes that the diffusion of the aforementioned elements have taken place at the interface. A proposed mechanism is that Ti reduces  $SiO_2$  at the interface producing  $Ti_2O_3$  or  $TiO$  and the free Si reacts with Ti to form the Ti complex compound  $Ti_5Si_3$  [35]. It might be expected that Ti reduces other oxides of porcelain with lower chemical affinity to O compared to Ti. This behaviour is commonly known as metallothermic reaction and is described by following formula:



where M stands for any metal. Among all the profiles tested only the Zr profile at the Ti–Triceram (paste) interface showed the maximum value at the Ti–ceramic interface. An explanation for this could be the segregation of Zr based particles at the interface during the firing of bonding agent. It is worthwhile to be noted that although Initial Ti and Triceram (paste) are delivered as single phase particles [33], they demonstrate a two phase structure as presented in Fig. 2c and h respectively. This behaviour might be readily explained by the nucleation and precipitation of new phases during firing of bonding agents.

There are several mechanical tests that have been used to determine the debonding strength between metal and porcelain and porcelain including a plethora of flexural and shear designs [27]. Generally the bond strength of metal–ceramic systems is evaluated with the three point bending according to ISO 9693:1999 [30] or with the shear testing. The latter although reliable, cannot be directly compared with the three point bending results. In some cases only the fracture mode has been used as a classification criterion [21,23,29] based on the former version of ISO 9693 standard, where metal–ceramic strips were bended over a rod to a  $90^\circ$  angle of the specimens ends. The specimens were then flattened and the percentage of adherent porcelain was determined along the predominant part of the middle third of the metallic substrate. The pass/fail criterion was that the adherent porcelain should cover more than 50% of the tested area implying that the fracture should be more than 50% cohesive within porcelain. However, it is obvious that such a test cannot provide qualitative results. The latest revision of ISO 9693 in 1999 based on the full adoption of the DIN 13927 [36] also commonly known as Schwickerath test [37]. According to this specification the metal–ceramic system comply with the requirements pass ISO 9693 when four out of six specimens have a debonding strength higher than 25 MPa [30].

Table 4 summarizes all the bond strength values found in relevant literature for the materials included in this study. The values are separated depending on the calculation methods. Although the three point bending has been applied in many cases, the calculation of bond strength has been inappropriately estimated employing the formulas for bending of uniform beams or maximum surface tensile stress [38]. Such erroneous approach has bond strength values up to 300 MPa [39] and thus all the values provided by the single beam theory will not be further evaluated. Further details for the mechanical theory bending of composite beams and mathematical

**Table 4 – Bond strengths values reported in literature for all the materials tested. The values are given in descending order (from left to right). The bond strength values that have been calculated based on ISO or three point flexural bending are given separately. Although the three point bending has been applied in many cases, the calculation of bond strength has been inappropriately estimated employing the formulas for bending of uniform beams or maximum surface tensile stress. The values of the present study are shown in bold format.**

Material	ISO 9693/DIN 13927/Schwickerath test										Flexural strength ( $\sigma = 3PL/2bd^2$ )		
TiKrom	45 ± 5												
Duceratin	42 ± 8	34 ± 4 [42]	32 ± 4 [16]	28 ± 3 [20]	17 ± 3 [31]							21 ± 3 [43]	
Initial Ti	31 ± 5												
Duceratin plus	31 ± 3	24 ± 1 [44]											
Ti-22	38 ± 3 [45]	36 ± 8 [18]	32 ± 5 [28]	29 ± 5	29 ± 2 [44]	25 ± 2 [14]						35 ± 8 [46]	
Triceram (paste)	28 ± 5 [45]	28 ± 3	27 ± 1 [44]									32 ± 4 [46]	
Triceram (powder)	23 ± 3 [31]	21 ± 4										39 ± 5 [48]	
TitanKeramik	37 ± 3 [47]	25 ± 4 [34]	21 ± 3	21 ± 3 [16]	19 ± 3 [14]							38 ± 2 [46]	25 ± 3 [49]
													25 ± 3 [22]

calculations for ISO formulas are given in previously published studies [38,39].

TiKrom showed the highest bond strength among materials tested with values comparable to modern Ni–Cr alloys [40]. The TiKrom bonding agent is a La–Ba based material [33] and the increased bond strength might be attributed to the beneficial effect of Ba content on Ti–porcelain joint [41]. Unfortunately, no comparable data for TiKrom and Initial Ti were found in the literature. Duceratin demonstrated a great variance in bond strength values ranging from 17 to 42 MPa. Two independent studies provided similar mean values of 34 and 32 MPa while the decrease in 28 MPa is appended to the firing conditions of porcelain layers in atmospheric air rather than conventional vacuum of dental ovens proposed for this treatment. However, there is no explanation for the very low value of 17 MPa apart from possible complications with the preparation of metal–ceramic specimens. The highest value for Duceratin is provided by the current study (although with high standard deviation) is difficult to be explained since Duceratin and Deceratin Plus bonding agents have slight differences in their elemental compositions [33]. Therefore the bond strength of Duceratin might have been overestimated in present study. Small differences were found for Duceratin Plus with the results of a previous study while the results for Ti-22 are within the range of reported values. Triceram (paste), Triceram (powder) and TitanKeramik showed very similar values with the results found in the literature (Table 4). The only exception is the 37 MPa value that is readily appended to the fact that the supportive span of the three point bending that used was different from that proposed by the ISO specification. It is also worthwhile to be noted that Triceram (paste) and TitanKeramik have almost similar values even among independent research studies, a behaviour that might be attributed to the fact that bonding agent in paste form are less technique sensitive and thus could provide more reproducible results among different dental laboratories. In general, these two materials showed less standard deviation compared to the porcelains with powder bonding agents. High standard deviations (6–10 MPa) were also found by a recent study [40] for many modern porcelains for precious and base dental alloys. Finally Triceram (powder) and TitanKeramik did not comply with ISO requirements.

According to fracture mode analysis Duceratin, Duceratin Plus, Ti-22, Triceram (powder) and Triceram (paste) demonstrated mainly adhesive fracture mode (Fig. 5 and Table 4) a finding that is in accordance with previous studies [31,32]. This type of fracture mode implies that the weakest mechanically joint is the Ti–porcelain interface. Statistical analysis showed that there was not correlation between the bond strength and the fracture mode. Although TiKrom and TitanKeramik demonstrated mainly cohesive fractures which is in accordance with previous findings [21–23,31,32] Tikrom yielded the highest bond strength and the TitanKeramik the lowest among the materials tested. This discrepancy can be caused by the great differences in cohesive strength of the bonding agents themselves. Two materials have completely different formulations. The bonding agent of TiKrom consists of La–Ba oxides while TitanKeramik is a silicon dioxide based material [33]. Additionally TitanKeramik demonstrates an intense porosity distribution whereas the bonding agent of Tikrom yields

a rather sound structure. Therefore it is readily explained that the fracture mode cannot be used for direct comparison among different porcelains.

Under the experimental conditions of the present study the materials tested showed great variations in bond strength and interfacial characteristics implying that the currently available low fusing porcelains might have also significant differences in their clinical behaviour.

## Acknowledgment

This study was granted by the Greek State Scholarships Foundation (IKY).

## REFERENCES

- [1] Kaus T, Probster L, Weber H. Clinical follow-up study of ceramic veneered titanium restorations—three-year results. *Int J Prosthodont* 1996;9:9–15.
- [2] Marklund S, Bergman B, Hedlund SO, Nilson H. An intraindividual clinical comparison of two metal–ceramic systems: a 5-year prospective study. *Int J Prosthodont* 2003;16:70–3.
- [3] Nakajima H, Okabe T. Titanium in dentistry: development and research in the U.S.A. *Dent Mater J* 1996;15:77–90.
- [4] Bergman B, Marklund S, Nilson H, Hedlund SO. An intraindividual clinical comparison of 2 metal–ceramic systems. *Int J Prosthodont* 1999;12:444–7.
- [5] Bergman B, Nilson H, Andersson M. A longitudinal clinical study of provera ceramic-veneered titanium copings. *Int J Prosthodont* 1999;12:135–9.
- [6] Walter M, Reppel PD, Boning K, Freesmeyer WB. Six-year follow-up of titanium and high-gold porcelain-fused-to-metal fixed partial dentures. *J Oral Rehabil* 1999;26:91–6.
- [7] Wang RR, Fenton A. Titanium for prosthodontic applications: a review of the literature. *Quintessence Int* 1996;27:401–8.
- [8] Eliopoulos D, Zinelis S, Papadopoulos T. The effect of investment material type on the contamination zone and mechanical properties of commercially pure titanium castings. *J Prosthet Dent* 2005;94:539–48.
- [9] Zinelis S. Effect of pressure of helium, argon, krypton, and xenon on the porosity, microstructure, and mechanical properties of commercially pure titanium castings. *J Prosthet Dent* 2000;84:575–82.
- [10] Lovgren R, Andersson B, Carlsson GE, Odman P. Prospective clinical 5-year study of ceramic-veneered titanium restorations with the Provera system. *J Prosthet Dent* 2000;84:514–21.
- [11] Adachi M, Mackert Jr JR, Parry EE, Fairhurst CW. Oxide adherence and porcelain bonding to titanium and Ti–6Al–4V alloy. *J Dent Res* 1990;69:1230–5.
- [12] Kimura H, Horng CJ, Okazaki M, Takahashi J. Oxidation effects on porcelain–titanium interface reactions and bond strength. *Dent Mater J* 1990;9:91–9.
- [13] Wang RR, Fung KK. Oxidation behavior of surface-modified titanium for titanium–ceramic restorations. *J Prosthet Dent* 1997;77:423–34.
- [14] Atsu S, Berksun S. Bond strength of three porcelains to two forms of titanium using two firing atmospheres. *J Prosthet Dent* 2000;84:567–74.
- [15] Pang IC, Gilbert JL, Chai J, Lautenschlager EP. Bonding characteristics of low-fusing porcelain bonded to pure titanium and palladium–copper alloy. *J Prosthet Dent* 1995;73:17–25.
- [16] Probster L, Maiwald U, Weber H. Three-point bending strength of ceramics fused to cast titanium. *Eur J Oral Sci* 1996;104:313–9.
- [17] Nilson H, Bergman B, Bessing C, Lundqvist P, Andersson M. Titanium copings veneered with provera ceramics: a longitudinal clinical study. *Int J Prosthodont* 1994;7:115–9.
- [18] Al Hussaini I, Al Wazzan KA. Effect of surface treatment on bond strength of low-fusing porcelain to commercially pure titanium. *J Prosthet Dent* 2005;94:350–6.
- [19] Kononen M, Kivilahti J. Bonding of low-fusing dental porcelain to commercially pure titanium. *J Biomed Mater Res* 1994;28:1027–35.
- [20] Yan M, Kao CT, Ye JS, Huang TH, Ding SJ. Effect of preoxidation of titanium on the titanium–ceramic bonding. *Surf Coat Technol* 2007;202:288–93.
- [21] Cai Z, Bunce N, Nunn ME, Okabe T. Porcelain adherence to dental cast CP titanium: effects of surface modifications. *Biomaterials* 2001;22:979–86.
- [22] Troia Jr MG, Henriques GE, Mesquita MF, Fragoso WS. The effect of surface modifications on titanium to enable titanium–porcelain bonding. *Dent Mater* 2008;24:28–33.
- [23] Sadeq A, Cai Z, Woody RD, Miller AW. Effects of interfacial variables on ceramic adherence to cast and machined commercially pure titanium. *J Prosthet Dent* 2003;90:10–7.
- [24] Yamada K, Onizuka T, Endo K, Ohno H, Swain MV. The influence of Goldbonder (TM) and pre-heat treatment on the adhesion of titanium alloy and porcelain. *J Oral Rehabil* 2005;32:213–20.
- [25] Yamada K, Onizuka T, Sumii T, Swain MV. The effect of Goldbonder on the adhesion between porcelain and pure titanium. *J Oral Rehabil* 2004;31:775–84.
- [26] Papadopoulos T, Tsetsekou A, Eliades G. Effect of aluminium oxide sandblasting on cast commercially pure titanium surfaces. *Eur J Prosthodont Restor Dent* 1999;7:15–21.
- [27] Hammad IA, Talic YF. Designs of bond strength tests for metal–ceramic complexes: review of the literature. *J Prosthet Dent* 1996;75:602–8.
- [28] Yoda M, Konno T, Takada Y, Iijima K, Griggs J, Okuno O, et al. Bond strength of binary titanium alloys to porcelain. *Biomaterials* 2001;22:1675–81.
- [29] Lee KM, Cai Z, Griggs JA, Guiatas L, Lee DJ, Okabe T. SEM/EDS evaluation of porcelain adherence to gold-coated cast titanium. *J Biomed Mater Res B Appl Biomater* 2004;68:165–73.
- [30] ISO 9693 Metal–ceramic dental restorative systems. Geneva: International Organization for Standardization; 1999.
- [31] Ozcan I, Uysal H. Effects of silicon coating on bond strength of two different titanium–ceramic to titanium. *Dent Mater* 2005;21:773–9.
- [32] Suansuwan N, Swain MV. Adhesion of porcelain to titanium and a titanium alloy. *J Dent* 2003;31:509–18.
- [33] Chakmakchi M, Eliades G, Zinelis S. Bonding agents of low fusing cpTi porcelains: elemental and morphological characterization. *J Prosthodont Res* 2009;53:166–71.
- [34] Inan O, Acar A, Halkaci S. Effects of sandblasting and electrical discharge machining on porcelain adherence to cast and machined commercially pure titanium. *J Biomed Mater Res B Appl Biomater* 2006;78:393–400.
- [35] Shevchencho N, Itin V, Tuhfatullin A. Reaction of stomatological porcelain with titanium and titanium nickelide during sintering. *Powder Metall Met C+* 2001;40:42–9.
- [36] DIN 13927 Metal–ceramic system: German Standard Institution Berlin. Beuth Verlag; 1990.

- [37] Lenz J, Schwarz S, Schwickerath H, Sperner F, Schafer A. Bond strength of metal–ceramic systems in three-point flexure bond test. *J Appl Biomater* 1995;6:55–64.
- [38] White SN, Ho L, Caputo AA, Goo E. Strength of porcelain fused to titanium beams. *J Prosthet Dent* 1996;75:640–8.
- [39] Derand T, Hero H. Bond strength of porcelain on cast vs. wrought titanium. *Scand J Dent Res* 1992;100:184–8.
- [40] Korkmaz T, Asar V. Comparative evaluation of bond strength of various metal–ceramic restorations. *Mater Des* 2009;30:445–51.
- [41] Oka K, Hanawa T, Kon M, Lee HH, Kawano F, Tomotake Y, et al. Effect of barium in porcelain on bonding strength of titanium–porcelain system. *Dent Mater J* 1996;15:111–20.
- [42] Zhang H, Guo TW, Li JM, Pan JG, Dang YG, Tong Y. Cr–Ti–Al–N complex coating on titanium to strengthen Ti/porcelain bonding. *Nan Fang Yi Ke Da Xue Xue Bao* 2006;26:154–7.
- [43] Ho WF, Chiang TY, Wu SC, Hsu HC. Mechanical properties and deformation behavior of cast binary Ti–Cr alloys. *J Alloy Compd* 2009;468:533–8.
- [44] Papadopoulos TD, Spyropoulos KD. The effect of a ceramic coating on the cpTi–porcelain bond strength. *Dent Mater* 2009;25:247–53.
- [45] Acar A, Inan O, Halkaci S. Effects of airborne-particle abrasion, sodium hydroxide anodization, and electrical discharge machining on porcelain adherence to cast commercially pure titanium. *J Biomed Mater Res B Appl Biomater* 2007;82:267–74.
- [46] Vasquez V, Ozcan M, Nishioka R, Souza R, Mesquita A, Pavanelli C. Mechanical and thermal cycling effects on the flexural strength of glass ceramics fused to titanium. *Dent Mater J* 2008;27:7–15.
- [47] Yilmaz H, Dincer C. Comparison of the bond compatibility of titanium and an NiCr alloy to dental porcelain. *J Dent* 1999;27:215–22.
- [48] Oyafuso DK, Ozcan M, Bottino MA, Itinoche MK. Influence of thermal and mechanical cycling on the flexural strength of ceramics with titanium or gold alloy frameworks. *Dent Mater* 2008;24:351–6.
- [49] Troia MG, Henriques GEP, Nobilo MAA, Mesquita MF. The effect of thermal cycling on the bond strength of low-fusing porcelain to commercially pure titanium and titanium–aluminium–vanadium alloy. *Dent Mater* 2003;19:790–6.